# DESIGN OF A THIN FILM CdTe SOLAR CELL

PETER V. MEYERS

*Ametek Applied Materials Laboratory, 352 Godshall Drive, Harleysville, PA 19438 (U.S.A.)*

## Summary

Cadmium telluride was originally considered for thin film solar cells because of its optimum band gap, high optical absorption coefficient and ability to be doped. Furthermore, it is a stable compound which can be produced by a wide variety of methods from stable raw materials. As thin film photovoltaics mature, however, it is clear that several more subtle attributes have a significant impact on the viability of commercialization. We discuss the observations which have provided insight and direction to Ametek's CdTe solar cell program. Rather than try to modify the inherent material properties of CdTe, advances have been made by designing a solar cell that exploits existing properties. Specifically, the tendency to self-compensate, which makes low resistance contacting difficult, is turned into an advantage in the n–i–p configuration; the CdTe provides an intrinsic layer with good carrier collection efficiency.

## 1. Introduction

Cadmium telluride has been shown to be the optimum material for photovoltaic (PV) devices not only from an analysis of the electrical and optical properties of the single crystal but from the results obtained on polycrystalline thin film devices. At least six groups have reported solar to electric conversion efficiencies of thin film CdTe devices above or near 10% [1 - 6]. A significant observation [7] is that these results have been obtained using CdTe which was produced by several completely different processes: electrodeposition, screen printing and close-spaced sublimation. Clearly, thin film CdTe has an innate tendency toward the electrical properties which are required to form high efficiency solar cells. (It may also be noted that thin film CdS exhibits a similar insensitivity to its method of production [8].) This characteristic may have great significance as CdTe solar cells reach the commercialization stage. Ametek intends to take full advantage of these and other properties of CdTe. The following, somewhat

anecdotal, description of our experience may provide further insight into our perspective

## 2. Metal–insulator–semiconductor (MIS) solar cells

Ametek's early solar cell used the MIS design: metal–insulator–semi-conductor. The process has been described in greater detail elsewhere [9], and only the basic construction of the device is described here. The CdTe is electroplated onto a cadmium film 1000 Å thick on nickel-clad stainless steel. After a heat treatment for 1 h at 310 °C in air, a 25 Å layer of aluminum oxide (the I layer) is deposited followed by a 200 Å layer of nickel (the M layer).

The heat treatment is of particular interest. Although all the device properties, $J_{sc}$, $V_{oc}$ and FF, were improved in heat-treated cells, the most dramatic effect was on the short-circuit current. For devices whose production did not include the heat treatment, $J_{sc}$ was of the order of 5 mA cm$^{-2}$; for devices whose production did include the heat treatment, $J_{sc}$ was of the order of 15 mA cm$^{-2}$. In order to determine the effect of the heat treatment on the material properties of the CdTe, films were bonded with epoxy to glass slides and then mechanically separated from the original substrate. The main effects observed were an increase in the dark resistivity, typically from $10^6$ ohm cm before to $10^8$ ohm cm after heat treatment, and a decrease in the prominence of a red tail in the photoconductivity spectrum. We interpreted these results as an annealing-out of electrically active defects in the CdTe. Thus the material was exhibiting its well-known tendency to self-compensate.

In separate experiments, p-type CdTe was produced by plating at a more positive potential [10]. After heat treating, however, the material became n type. Many factors may have contributed to this conversion, *e.g.* the cadmium underlayer, the heat treatment ambient, enhanced diffusion at grain boundaries or impurities incorporated in the deposit, whatever the cause, the conversion did occur. Although the CdTe was not intentionally doped, following the heat treatment it behaved like a high resistivity n-type semiconductor.

Thus, although a heat treatment is necessary to produce high quality thin film CdTe, this same heat treatment can change the effective carrier concentration and even the dominant carrier type of the film. This result suggests that thin film CdTe is most appropriate when used in conjunction with other materials, *i.e.* in either the heterojunction or the MIS configuration. One oft-touted attribute of CdTe is its ability to be produced as either n type or p type; the self-compensation tendency may account for the absence of any high efficiency thin film p–n homojunction.

We observed that the highest efficiency cells were constructed of high resistivity CdTe, presumably because this was also the highest quality CdTe One problem often encountered in working with high resistivity material

is that it is difficult to make low resistance ohmic contacts. In this case, however, low resistance contact is made through the cadmium underlayer. Another manifestation of the high resistivity was the observation of photo-generated majority-carrier effects [11]. In this case holes generated by the light diffuse against the electric field in the space charge region and into the metal layer. This shows up as (a) a lowered response in the blue portion of the quantum efficiency spectrum with respect to that observed in the red portion, (b) a significant deviation from the superposition principle and (c) a saturation of the open-circuit voltage with intensity which is observed at low temperatures. In this design the photogenerated majority effects were reduced by proper passivation of the semiconductor–insulator interface. It is clear, however, that any solar cell design must consider the effect of photogenerated carriers diffusing against the relatively weak electric field in the space charge region.

The two primary problems associated with the MIS devices were that (a) the built-in voltage was limited by interface states to a value of approximately 0.9 V and (b) the optical transmission of the nickel layer was approximately 70%. This latter limit was established by the competing requirement for high electrical conductivity along the metal layer. Thus the most efficient MIS device produced had a $V_{oc}$ of 0.723 V, a $J_{sc}$ of 18.7 mA cm$^{-2}$ and an efficiency of 8.6% [12].

### 2 1 Heterojunctions

These limitations on voltage and current can be overcome in the hetero-junction structure [13, 14]. The diffusion voltage of a CdTe/CdS junction is predicted to be 1.02 V; by substituting $Cd_{0.65}Zn_{0.35}S$ for CdS, the diffusion voltage can be increased to 1.22 V. The current over the MIS design can be increased by using transparent conducting oxides (TCO) and a thin $Cd_{1-x}Zn_xS$ window as the top surface of the device.

### 2.2. CdS/CdTe fabrication procedure

The substrate for these solar cells is commercially available $SnO_2$- or ITO-coated glass. CdS is deposited by pyrolysis at a temperature of 450 °C from an aqueous mist containing dissolved $CdCl_2$ and thiourea; a typical film thickness is 0.15 $\mu$m. CdTe is electroplated as in the MIS design to a thickness of 2 $\mu$m. This step is followed by a heat treatment in air for 20 min at approximately 400 °C. The CdTe surface is then etched in a mild solution of bromine–methanol. Vacuum-evaporated gold is used to complete the device. Devices larger than 10 mm$^2$ require conductive fingers which are made with a silver or nickel paste.

### 2.3. CdS/CdTe device properties

Heterojunction cells have indeed delivered higher currents and voltages than MIS cells produced from the same material. A 4 cm$^2$ cell produced as above exhibited a $J_{sc}$ of 22 mA cm$^{-2}$, a $V_{oc}$ of 740 mV and an efficiency of

10.4% [1] Furthermore, we have observed a $V_{oc}$ of 824 mV on a dot cel (8 mm$^2$).

### 2.4 n–i–p solar cells

The main problems associated with p-CdTe based heterojunctions have been [7]: (a) the difficulty of preparing high conductivity films, (b) the difficulty of making low resistivity contacts and (c) low minority-carrier lifetimes. As noted above, these problems have not prevented researchers from producing solar cells with efficiencies in excess of 10%, but most of these results have been obtained using gold contacts to the p-CdTe. Gold diffuses readily in CdTe, however, and these contacts are not expected to be stable over the desired 20 - 30 year life of a solar cell. In spite of encouraging results reported by Matsushita [15] using copper-doped sintered carbon, the search for improved low resistivity stable contacts to p-CdTe continues.

Rather than wrestle with the difficult problems of changing the properties of thin film CdTe, the n–i–p solar cell being developed at Ametek [1] is designed to accommodate its innate properties. As can be seen in the idealized energy-band diagram shown in Fig. 1, high resistivity rather than low resistivity films are desired; rectification rather than low resistance contacts are employed, and the collection of charge carriers is assisted by the field in the i layer In addition, even in the absence of doping, CdS is n type and ZnTe is p type; thus each material is utilized in its most easily prepared type.

Furthermore, the literature values of the electron affinity and band gap predict that there will be a minimal discontinuity in the valence band edge at the CdTe/ZnTe interface [16], thus permitting free flow of holes from the CdTe into the ZnTe. Likewise, at the CdTe/CdS interface there is no barrier to the flow of electrons into the CdS, and this remains true when zinc is substituted for up to 35% of the cadmium [13]. However, there are substantial barriers to the flow of electrons into the ZnTe and of holes into the CdS.
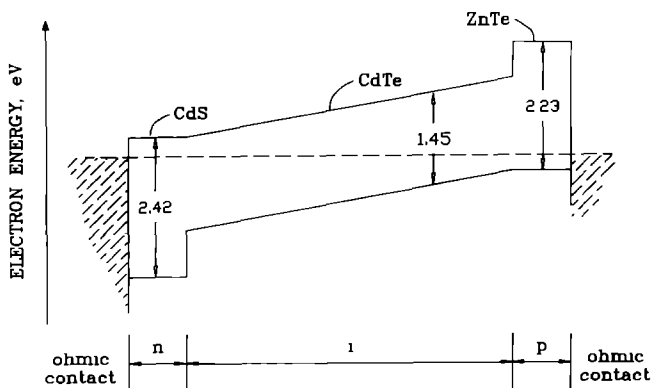


Fig. 1 Idealized energy band diagram of the CdS/CdTe/ZnTe n–i–p solar cell.

CdS and ZnTe are both wide band gap semiconductors suitable as the window layer; therefore the device may be constructed with the light entering from either side. More importantly, since the entire device is transparent to subband gap radiation, it is ideal as the top cell in a cascade design [1].

### 2.5. n–i–p fabrication procedure

Fabrication procedures for the n–i–p solar cell are similar to those for the CdS/CdTe heterojunction except that a 0.06 $\mu$m layer of ZnTe is vacuum evaporated onto a 250 °C surface of CdTe etched in bromine–methanol. In addition, the choice of back-contact metal is not limited to gold; nickel also produces good contacts.

### 2.6 Design flexibility

The CdS/CdTe/ZnTe configuration alone is not sufficient to produce high efficiency n–i–p solar cells. Subtle changes in the process can be shown to have a significant effect on device properties. This is demonstrated in the electron-beam-induced current (EBIC) and spectral response data from devices displayed in Fig. 2. Both devices have the same nominal configuration, yet each exhibits distinctively different characteristics. While these differences arise from variations in the fabrication procedure, the detailed relationships among process steps are the topics of current investigations. The data are presented only to demonstrate the flexibility and design possibilities of this structure.

Device A was constructed as above except that the CdTe heat treatment was carried out at 300 °C in flowing nitrogen gas and the ZnTe was deposited onto a substrate heated to 150 °C. The fabrication of device B varied from the standard procedure in that the substrate was heated to 200 °C during ZnTe deposition. The air mass (AM) 1 current–voltage ($I$–$V$) curves and spectral response were measured with illumination from each of the CdS and ZnTe sides, and the EBIC signal generated in a cross-section of each device was recorded.

Device A has its maximum field strength at the CdTe/ZnTe junction. This is suggested by the AM 1 data listed in Table 1, but is most evident from the EBIC signal, which exhibits its maximum intensity near this interface. Likewise, the spectral response recorded from the CdS side shows only a small peak at the long-wavelength end of the spectrum (where light is weakly absorbed and can penetrate to the CdTe–ZnTe interface), while the spectral response from the ZnTe side is strong over the region from the absorption edge of the ZnTe to that of the CdTe. Device B is in many ways the inverse of A: the $J_{sc}$ is higher and the spectral response is stronger over a wider region when the device is illuminated from the CdS side, and the EBIC signal peaks near the CdS/CdTe interface. While neither of these devices has been optimized for high efficiency, they exemplify the range of characteristics available.
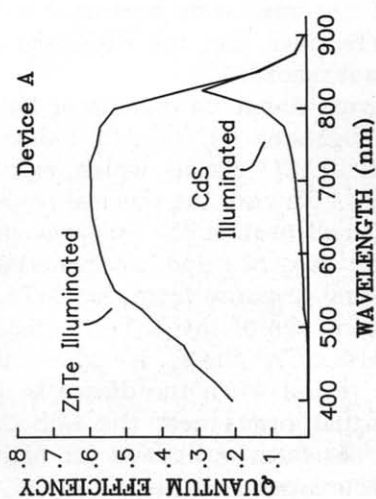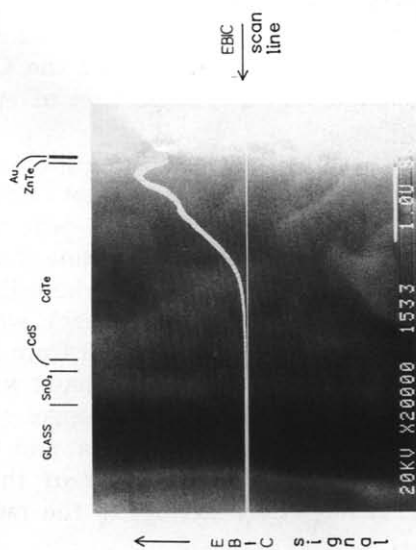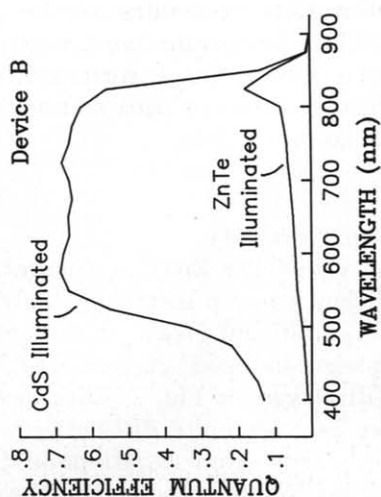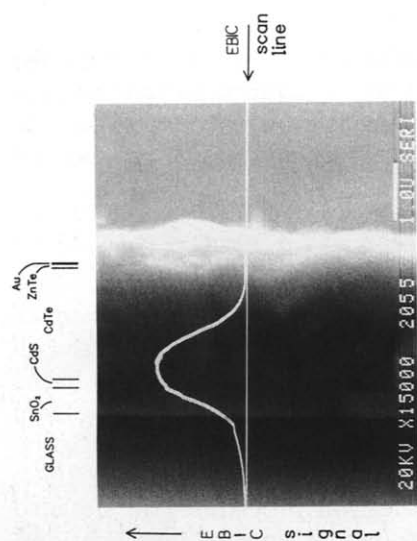
Fig. 2. Spectral response and EBIC data from two CdS/CdTe/ZnTe solar cells produced with variations from the standard process: (a) device A, heat treated at 300 °C in flowing nitrogen and ZnTe deposited at 300 °C, (b) device B, ZnTe deposited at 200 °C.

TABLE 1

Device properties of devices A and B under simulated AM 1 illumination from each side of the solar cell

|  | Device A | Device B |
|---|---|---|
| *Illumination from the CdS side* | | |
| $V_{oc}$ (mV) | 472 | 698 |
| $J_{sc}$ (mA cm$^{-2}$) | 0 8 | 22.1 |
| FF | 0.36 | 0.56 |
| *Illumination from the ZnTe side* | | |
| $V_{oc}$ (mV) | 641 | 607 |
| $J_{sc}$ (mA cm$^{-2}$) | 11.6 | 2.6 |
| FF | 0.58 | 0.45 |

An n–i–p device produced using the standard procedures has the EBIC signal shown in Fig. 3. This device had an efficiency of 10.4% with $J_{sc}$ = 22.3 mA cm$^{-2}$, $V_{oc}$ = 718 mV and FF = 0.65. It appears that the maximum field strength occurs at a depth of approximately 0.5 $\mu$m from the CdS/CdTe junction and that the greater portion of the CdTe is active. This model of a wide depletion- width is supported by capacitance measurements which indicate a depletion width of the order of magnitude of the CdTe thickness. Thus, although this device may not have the idealized band diagram shown in Fig. 1, it is clearly an n–i–p solar cell.

### 2.7. n–i–p device properties

One submodule consisting of ten solar cells, each with an area of 5.1 cm$^2$, was constructed as above using nickel for the back-contact metal. The cells were first electrically isolated by mechanically scribing through
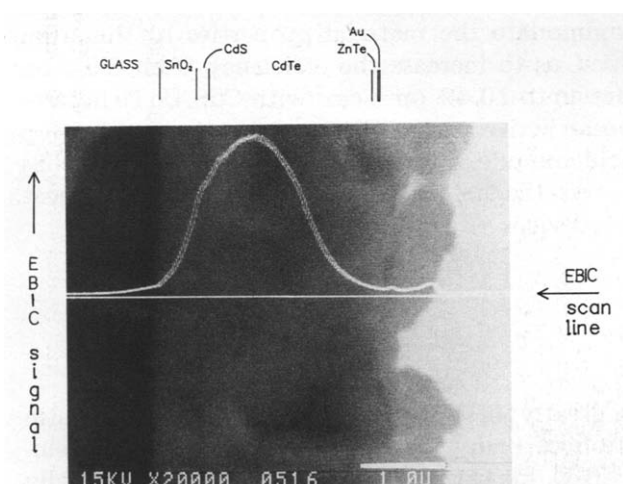


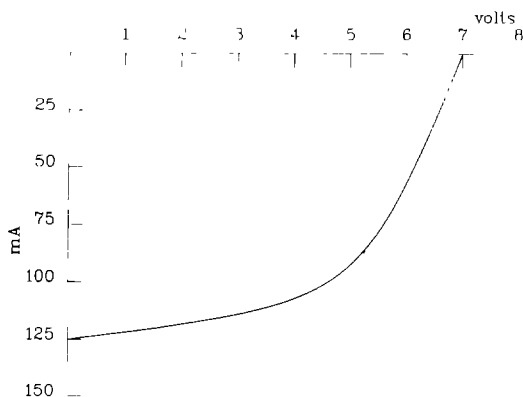Fig. 3. EBIC data from a standard n–i–p solar cell.

Fig. 4. Current–voltage characteristics of a proof-of-concept CdS/CdTe/ZnTe n–i–p solar module (10 cell module, each cell of area 5.10 cm$^2$; cell area ratio, about 0.66, substrate size, 3 in × 6 in): active-area efficiency, 9.3%; total-area efficiency, 6 1%; $I_{sc}$ = 125 mA; $J_{sc}$ = 24.5 mA cm$^{-2}$; $V_{oc}$ = 7.0 V; FF = 0.54.

the ITO layer. Then the cell edges were covered with a screen-printed insulator and interconnected with evaporated aluminum covered with silver paste. The AM 1 $I$–$V$ curve is shown in Fig. 4. The submodule had a $V_{oc}$ of 7.0 V, and $I_{sc}$ of 125 mA and a FF of 0.54. The active-area efficiency was 9.3%; the area ratio, i.e. the ratio of the active to the total area, was 0.66. We expect to see improvement in future devices; separate results obtained on 8 mm$^2$ dot cells produced a $V_{oc}$ of 774 mV and a FF of 0.75.

## 3. Conclusion

This article discusses the design changes in Ametek's solar cells which were made in order to accommodate the material properties of thin film CdTe. This strategy has helped us to increase the efficiency from 8.6% on 2 mm$^2$ dot cells of the MIS design to 10.4% on 4 cm$^2$ with CdS/CdTe hetero-junction cells and to 9.3% on an active area of 51 cm$^2$ using the novel n–i–p structure in a proof-of-concept module. Furthermore, the n–i–p design has several potential advantages over the heterojunction design and we expect to capitalize on these in future devices.

# References

1 P. V Meyers, *Proc. 7th Commission of the European Communities Conf. on Photovoltaic Solar Energy, 1986*, Reidel, Dordrecht, 1986, pp. 1211 - 1213.
2 H. Matsumoto, K. Kuribayashi, H. Uda, Y. Komatsu, A. Nakano and S. Ikegami, *Sol. Cells, 11* (1984) 367.
3 Y Tyan and E A. Perez-Albuerne, *Proc. 16th IEEE Photovoltaic Specialists' Conf, San Diego, CA, 1982*, IEEE, New York, 1982, pp. 794 - 800.
4 K. W. Mitchell, C. Eberspacher, F. Cohen, J. Avery, G. Duran and W. Bottenberg, *Proc. 18th IEEE Photovoltaic Specialists' Conf., Las Vegas, NV, 1985*, IEEE, New York, 1985, pp. 1359 - 1364.
5 T L. Chu, S. S. Chu and S T. Ang, *Proc. 19th IEEE Photovoltaic Specialists' Conf., New Orleans, LA, 1987*, IEEE, New York, 1987, pp. 1466 - 1469.
6 B M. Basol, *J. Appl. Phys., 55* (1984) 601.
7 R H Bube, in J. A. Amick, V. K. Kapoor and J. Dietl (eds.), *Proc. Symp. on Materials and New Processing Technol for Photovoltaics*, Vol 83-11, Electrochemical Society, Pennington, NJ, 1983, p. 359.
8 T. J. Coutts, *Thin Solid Films, 90* (1982) 451 - 460.
9 G. Fulop, J. Betz, P. Meyers and M. Doty, *U.S. Patents 426 04 27, 1981; 426 18 02, 1981; 434 51 07, 1982*.
10 M. P. R. Panicker, M. Knaster and F. A. Kroger, *J. Electrochem. Soc., 125* (4) (1978) 566 - 572.
11 S. M. So, W. Hwang, P. Meyers and C. H. Liu, *J. Appl. Phys., 55* (1) (1984) 253 - 261, *IEEE Trans. Electron Devices, 31* (5) (1984) 696 - 707.
12 G. Fulop, M. Doty, P Meyers, J. Betz and C. H. Liu, *Appl. Phys. Lett., 40* (4) (1982) 327 - 328.
13 A. L. Fahrenbruch, V. Vasilchenko, F. Buch, K. Mitchell and R. H. Bube, *Appl. Phys. Lett., 25* (10) (1974) 605 - 608.
14 S. Yin, A. Fahrenbruch and R. H. Bube, *J. Appl. Phys., 49* (3) (1978) 1294 - 1296.
15 A. Nakano, S. Ikegami, H. Matsumoto, H. Uda and Y Komatsu, *Sol. Cells, 17* (1986) 233 - 240.
16 J Tersoff, *Phys. Rev. Lett., 56* (25) (1986) 2755 - 2758.